Biochemical and Biophysical Research Communications 444 (2014) 562–567

Contents lists available at ScienceDirect

Biochemical and Biophysical Research Communications

journal homepage: www.elsevier.com/locate/ybbrc

Engineering micropatterned surfaces to modulate the function of vascular stem cells

Jennifer Li [a,1], Michelle Wu [a,1], Julia Chu [a], Ryan Sochol [b], Shyam Patel [a,*]

[a] Department of Bioengineering, University of California, Berkeley, 121 Stanley Hall, Berkeley, CA 94720, United States
[b] Berkeley Sensor and Actuator Center, University of California, Berkeley, 668 Sutardja Dai Hall, Berkeley, CA 94720, United States

ARTICLE INFO

Article history:
Received 30 December 2013
Available online 29 January 2014

Keywords:
Vascular stem cells
Cardiovascular
Micropatterning
Microposts
Microgrooves

ABSTRACT

Multipotent vascular stem cells have been implicated in vascular disease and in tissue remodeling post therapeutic intervention. Hyper-proliferation and calcified extracellular matrix deposition of VSC cause blood vessel narrowing and plaque hardening thereby increasing the risk of myocardial infarct. In this study, to optimize the surface design of vascular implants, we determined whether micropatterned polymer surfaces can modulate VSC differentiation and calcified matrix deposition. Undifferentiated rat VSC were cultured on microgrooved surfaces of varied groove widths, and on micropost surfaces. 10 μm microgrooved surfaces elongated VSC and decreased cell proliferation. However, microgrooved surfaces did not attenuate calcified extracellular matrix deposition by VSC cultured in osteogenic media conditions. In contrast, VSC cultured on micropost surfaces assumed a dendritic morphology, were significantly less proliferative, and deposited minimal calcified extracellular matrix. These results have significant implications for optimizing the design of cardiovascular implant surfaces.

1. Introduction

Cardiovascular disease is the leading cause of death in the United States. Coronary Artery Disease (CAD), a narrowing of the coronary arteries caused by plaque and inflammation, accounts for 16% of deaths and $108.9 billion in healthcare costs annually in the US. Plaque hardening, caused by osteoblastic deposition of calcified matrix, significantly increases the risk of plaque rupture, inflammation and, ultimately, myocardial infarct [1]. Furthermore, balloon angioplasty and stenting treatments to restore arterial patency cause vessel wall injury and can result in arterial narrowing from tissue restenosis. Even in the era of drug eluting stents, tissue restenosis remains a major complication of CAD treatment [2]. Second generation drug eluting stents, although significantly more effective than bare metal or first general drug eluting stents, still suffer from a restenosis rate of 12.2% [3].

The traditional model of vascular disease held that de-differentiated smooth muscle cells were responsible for intimal thickening in atherosclerosis, and for tissue restenosis following angioplasty and stenting. Furthermore, smooth muscle cells were implicated in calcified matrix formation in diseased arteries [4]. However, more recently, a population of multipotent vascular stem cells (VSCs) was found resident in the blood vessel wall [5]. In response to vascular injury, VSCs were shown to differentiate and contribute to vascular remodeling, to structural changes involving media thickening, and to reduced vessel lumen diameter. The VSC were also shown to be capable of osteogenic differentiation *in vitro*. Thus, it may be likely that VSC not only are responsible for vessel wall thickening but also for tissue calcification. Given the proliferative and differentiation potential of VSC, there is a critical clinical need to develop therapeutics that specifically target VSC function. Modulation of VSC behavior may lead to drastically improved clinical outcomes by preventing or limiting arterial narrowing and hardening.

Micro- and nano-topographic patterned biomaterial surfaces have been studied for biophysical regulation of cell functions such as orientation, proliferation, differentiation and tissue formation [6–13]. In particular, microgrooved surfaces have been shown to reduce vascular smooth muscle cell proliferation. Additionally, micropost substrates with varying micropost stiffness modulated human mesenchymal stem cell morphology, proliferation and differentiation [14], and directed endothelial cell migration [15]. In this study, we assessed the effect of microgrooves and microposts on rat vascular stem cell proliferation, osteogenic differentiation, and calcified matrix deposition.

* Corresponding author.
E-mail address: shyampatel@berkeley.edu (S. Patel).
[1] These authors contributed equally to this work.

http://dx.doi.org/10.1016/j.bbrc.2014.01.100
0006-291X/

2. Materials and methods

2.1. VSC culture

Primary rat VSCs were obtained by using aorta tissue explant culture as previously described [5]. VSC cultures were maintained with Dulbecco's modified Eagle's medium (DMEM) supplemented with 10% fetal bovine serum (FBS) and 1% penicillin/streptomycin (PS) (complete medium) in an incubator at 37 °C. Cell cultures were maintained in a humidified 95% air–5% CO_2 incubator at 37 °C.

2.2. Micropatterned PDMS membranes

Polydimethylsiloxane (PDMS) membranes with micropatterned grooves and micropatterned posts were fabricated as previously described [8,13,15]. The PDMS was spun-coated onto photolithography patterned silicon wafers with appropriate microgrooves of various widths (10, 50, and 100 μm) and 3 μm depth, or with uniformly distributed cylindrical micropits of 7 μm depth, 3 μm diameter and 3 μm spacing. The PDMS was cured by baking on a hotplate, and the PDMS membrane was removed and cut to appropriate sizes. As an experimental control, unpatterned PDMS membranes were spun-coated and cured on a silicon wafer with a smooth surface. PDMS membranes were sterilized and coated with Cellstart (Life Technologies, Grand Island, NY) prior to rat VSC culture.

2.3. Immunofluorescence staining of VSC mutlipotency markers

Rat VSC were characterized for multipotency markers as previously described [5]. Rat VSC were immunofluorescently stained for Sox10 (R&D Systems, Minneapolis, MN) and Neurofilament-M (Abcam, Cambridge, MA), and counter-stained with DAPI (Sigma–Aldrich, St. Louis, MO). The samples were imaged with a Zeiss fluorescent microscope (Zeiss).

2.4. Morphological assessment of VSC on micropatterned membranes

Rat VSC morphology on micropatterned membranes was analyzed with fluorescent staining of the actin cytoskeleton. Rat VSC were cultured on the micropatterned and control PDMS membranes for 24 h. After 24-h culture the cells were fixed, permeabilized and fluorescently stained with Alexa Fluor 546 phalloidin (Life Technologies, Grand Island, NY) and DAPI. The fluorescently stained samples were imaged with the Zeiss fluorescent microscope.

2.5. VSC proliferation on micropatterned membranes

The effect of micropatterned surfaces on rat VSC proliferation was measured using the Click-It 5-Ethyl-2′-deoxyuridine (EdU) proliferation assay (Life Technologies, Grand Island, NY). Rat VSC were cultured on micropatterned and control PDMS membranes for 48 h in complete medium.

After 48 h culture in complete medium, the rat VSC were pulsed with EdU for 1 h. The cells were then fixed, permeabilized, and fluorescently stained. For EdU detection cells were incubated with Alexa Fluor azide 488, and then counter-stained with DAPI. The stained samples were imaged with a Zeiss Fluorescence microscope. The images of EdU and DAPI staining were used to count proliferative cells and total number of cells using ImageJ software. Proliferation rate for each surface treatment was determined as the percentage of cells incorporated with EdU.

2.6. Osteogenic differentiation of VSC on micropatterned membranes

Rat VSC were cultured on micropatterned and control PDMS membranes in complete medium until 70% confluence. The cultures were then switched to osteogenic induction media and cultured for 4 weeks to induce osteogenic differentiation and calcified matrix deposition as described previously [5].

Osteogenic differentiation of and calcified matrix deposition by rat VSC on the micropatterned surfaces was assessed with alizarin red staining. Alizarin red complexes with calcium and produces a bright red/orange stain that can be imaged with light microscopy. Alizarin red solution was prepared by mixing 1 g of Alizarin Red S in 50 mL distilled water and adjusted to pH 4.3 using 10% ammonium hydroxide. The micropatterned and control samples were washed with PBS and then incubated with Alizarin Red for 20 min. After staining, the cells were washed with distilled water and then imaged with a Zeiss light microscope.

2.7. Statistical analysis

One-way ANOVA with post-hoc Tukey's multiple comparison (95% confidence interval) was used to determine significant differences in proliferation rates between surface treatments.

3. Results and discussion

3.1. Rat VSC expressed pluripotency markers

We first examined the effects of parallel microgrooves on rat VSC morphology, proliferation and osteogenic differentiation. All experiments were conducted with low passage, undifferentiated rat aortic VSC. Rat VSC multipotency was verified by immunofluorescent staining of Sox10 and NFM. As shown in Fig. 1, all cells expressed Sox10 and NFM. Diffuse staining of NFM was observed in the cell cytoplasm (Fig. 1B). Sox10, a transcriptional factor, was primarily localized in the nucleus (Fig. 1C and D). The Sox10 and NFM staining profile, consistent with previous results [5], suggested that VSCs in culture were in an undifferentiated state.

3.2. 10 μm microgrooved surfaces constricted and oriented VSC

Microgrooved PDMS membranes composed of parallel alternating ridges and grooves were produced with groove and ridge widths of 10, 50 or 100 μm (Fig. 2). To assess the effects of parallel microgrooves on VSC morphology, the cells were cultured on 10, 50 and 100 μm microgrooved PDMS membranes (Fig. 2). Actin cytoskeletal staining with fluorescent phalloidin showed that cell morphology was guided by the topography of the micropatterned surfaces. VSC cultured on control surfaces had flat, spread morphology with no particular cytoskeletal or nuclear orientation. On the microgrooves, VSCs generally exhibited an elongated morphology and cytoskeletal alignment parallel to microgroove orientation. On the 10 μm width microgrooves, the cellular actin cytoskeleton and membrane protrusions were aligned along the pattern direction (Fig. 2B). On the wider patterned surfaces (50 and 100 μm), the cellular actin cytoskeleton and membrane protrusions showed a partial alignment with the microgrooves, resulting in less cell elongation than that on narrower microgrooves (Fig. 2C and D). Overall cell size, however, was similar on all cell surfaces thereby indicating that the cells spanned across channels on the smaller widths.

The results of these morphological studies suggest that the smaller 10 μm microgrooves were more effective in orienting VSC actin cytoskeleton and membrane protrusion parallel to the

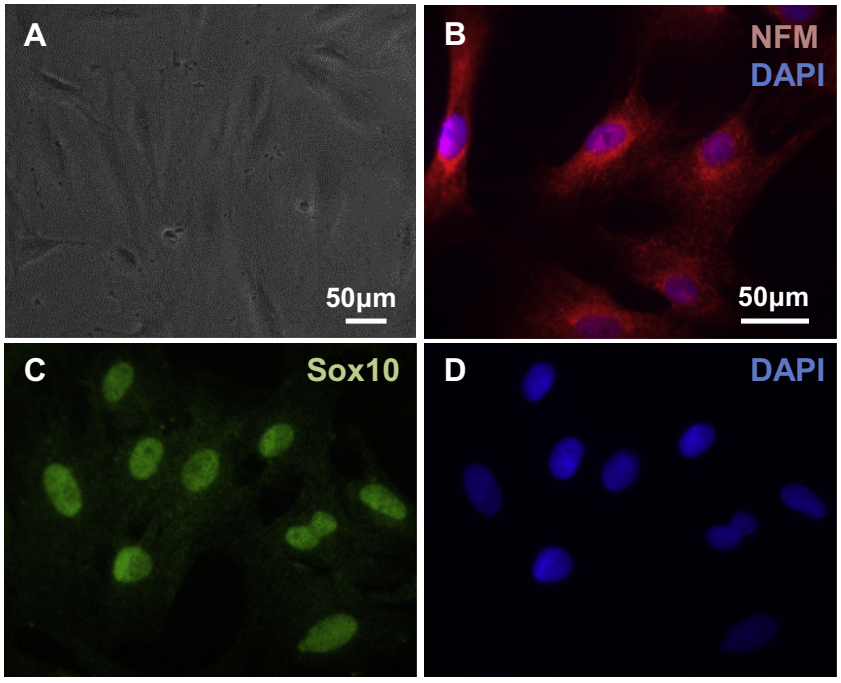

Fig. 1. Characterization of VSC culture. (A) Phase contrast image of VSCs. VSC were stained for multipotency markers. Characteristic diffuse NFM staining was observed in cultured cells (B). Nuclear Sox-10 staining was also observed in cultured cells (C, DAPI counterstaining in D). Scale Bar = 50 μm.

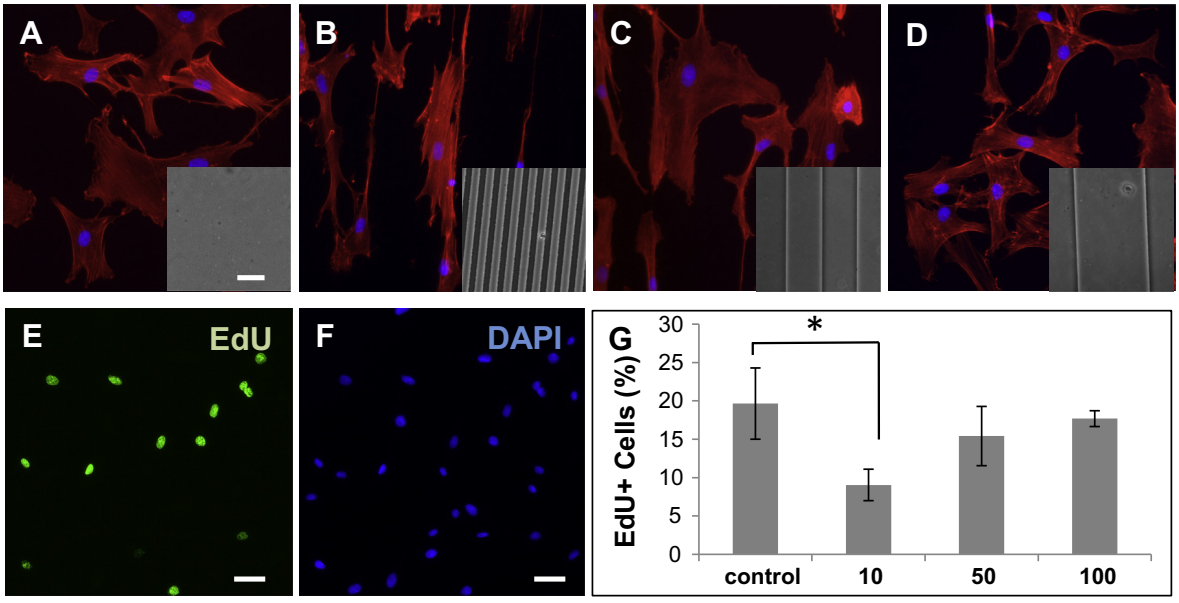

Fig. 2. VSC morphology and proliferation on control and microgrooved PDMS substrates. Alexa 546 Phalloidin fluorescently stained actin in VSC cultured on control (A), and on 10 μm (B), 50 μm (C) and 100 μm (D) microgrooved PDMS. Cell nuclei were counterstained with DAPI. Phase contrast insets show PDMS morphology. Cell proliferation was assessed using EdU incorporation assay. Incorporated EdU was fluorescently stained with Alexa Azide 488 (E). All cell nuclei were counterstained with DAPI (F). Percentage of EdU positive cells on control and microgrooved surfaces was quantified (G). Scale bar = 50 μm. $^{*}p < 0.05$ compared to control.

pattern direction. This result is consistent with previously reported results with other cell types cultured on similarly dimensioned microgroove surfaces [9,13,16].

3.3. 10 μm microgrooved surfaces reduced VSC proliferation

Next, we determined whether the microgrooved surfaces modulated VSC proliferation by using the EdU incorporation assay (Fig. 2E and F). Compared to the control surface, cells cultured on 10 μm microgrooves showed a significant decrease in proliferation (20% on control vs. 9% on 10 μm microgrooves) (Fig. 2G). Cell proliferation on 100 and 50 μm microgrooved surfaces was not significantly different from the control surface. Previous studies on single cell patterning of smooth muscle and mesenchymal stem cells have shown that constriction of the cell nucleus and cytoskeleton results in lower cell proliferation [8,13]. These results suggest that the elongated VSC morphology induced by the 10 μm microgrooves is sufficient to shift the VSC toward a less proliferative phenotype. *In vivo*, microgrooved implants may prevent VSC hyper-proliferation via a biophysical mechanism thereby reducing

tissue restenosis and blood vessel constriction. Thus, microgroove patterning of cardiovascular implants, such as stents, may serve as a safer alternative to cytostatic drug elution.

3.4. VSC underwent osteogenic differentiation on microgrooved surfaces

We then investigated the effects of microgrooved surfaces on rat VSC osteogenic differentiation and calcified matrix deposition. VSC were cultured on control and microgrooved surfaces for 4 weeks in osteogenic differentiation medium. Calcified matrix deposition by VSC on the various surfaces was assessed with alizarin red staining. Similarly to Wang et al. [5], VSC on control PDMS surfaces differentiated toward the osteogenic lineage and deposited calcified matrix (Fig. 3A). The 10 μm width microgrooves also showed high intensity of alizarin red staining, similar to the control surface (Fig. 3B). Microgrooves of widths at 50 and 100 μm showed lower intensity and more diffuse alizarin red staining and a higher density of unstained cells (Fig. 3C and D).

The alizarin red staining results suggest that the 10 μm width microgrooves facilitate calcified matrix deposition while the wider microgroove surfaces at least partially suppress such deposition. Previous studies have generally shown that osteogenic differentiation of mesenchymal stem and progenitor cells is dependent on cell spreading and cell-substrate interactions. Single cell patterning studies have shown that osteogenic differentiation is enhanced with increased cell spreading area [17]. Similarly, studies of mesenchymal progenitor cells cultured on microgrooved and nanopatterned surfaces suggested that optimal cell-substrate adhesion and formation of long focal adhesions are required for osteogenic differentiation [12,18,19]. Our results with the microgroove surfaces differed from previous studies in that the cells cultured on narrower widths showed robust osteogenic differentiation and calcified matrix deposition. This discrepancy may be due to differences in microgroove depth. The previous studies utilized depths of 500 nm or less while this study utilized groove depths of 3 μm. The large step size may have disrupted cell-substrate interactions on the wider 50 and 100 μm microgrooves. In contrast, the cells cultured on 10 μm microgrooves were oriented along and spread across the ridge surfaces, and this spreading behavior may have formed more stable focal adhesion complexes.

Overall, while the 10 μm microgrooved surface was effective in reducing VSC proliferation it did not suppress calcified matrix deposition from osteogenic VSC. Thus, while the 10 μm micrgrooved surface may aid in the reduction of tissue restenosis on cardiovascular implants it may not be effective in preventing tissue calcification.

3.5. VSC cultured on micropost surfaces demonstrated dendritic morphology

We then hypothesized that a micropost patterned surface could be effective in reducing both VSC proliferation and calcified matrix deposition by constricting cell shape and disrupting focal adhesion formation, respectively. We fabricated micropost structures with 7 μm height, 3 μm diameter and 3 μm spacing on PDMS membranes (Fig. 4A). VSC cultured on microposts displayed dendritic morphology with various filopodia spanning across multiple adjacent microposts (Fig. 4B). The cells displayed no particular cytoskeletal or nuclear orientation on the micropost surfaces. These results suggest that the microposts effectively reduced the available surface area for integrin adhesion and focal adhesion complex formation. In addition, the regularity and spacing of the microposts enabled the cells to extend long filopodia.

3.6. Micropost surfaces decreased VSC proliferation

We then determined whether the constricted morphology on microposts affected VSC proliferation. VSC proliferation on micropost and control surfaces was assessed using EdU assay. Micropost surfaces significantly reduced VSC proliferation as compared to control surfaces (20% on control vs. 8% on microposts) (Fig. 4C).

Previous studies have reported mixed results of the effect of microposts on cell proliferation. Green et al., showed decreased

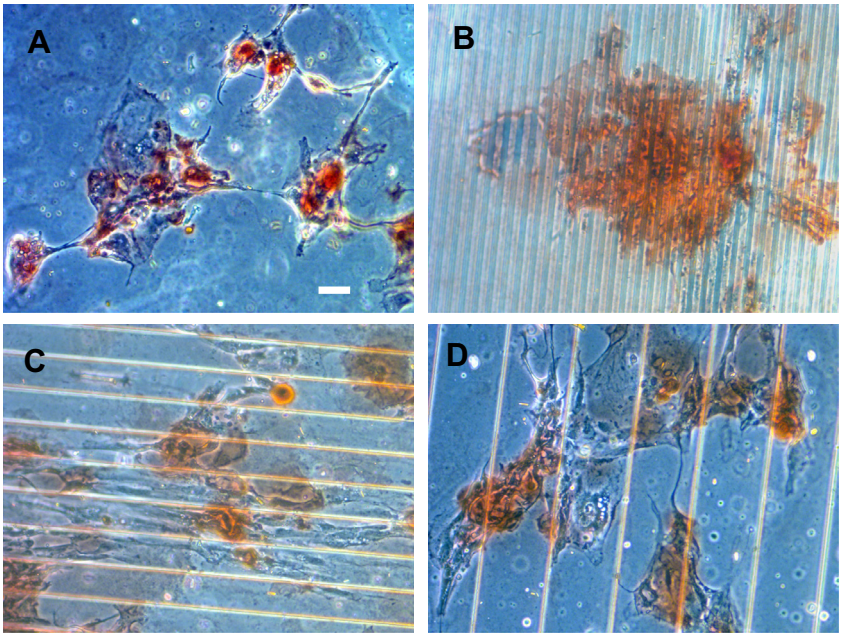

Fig. 3. Alizarin red staining of calcified matrix deposition by VSC cultured in osteogenic media conditions on control (A) and 10 μm (B), 50 μm (C) and 100 μm (D) microgrooved PDMS substrates. Scale bar = 50 μm. (For interpretation of the references to color in this figure legend, the reader is referred to the web version of this article.)

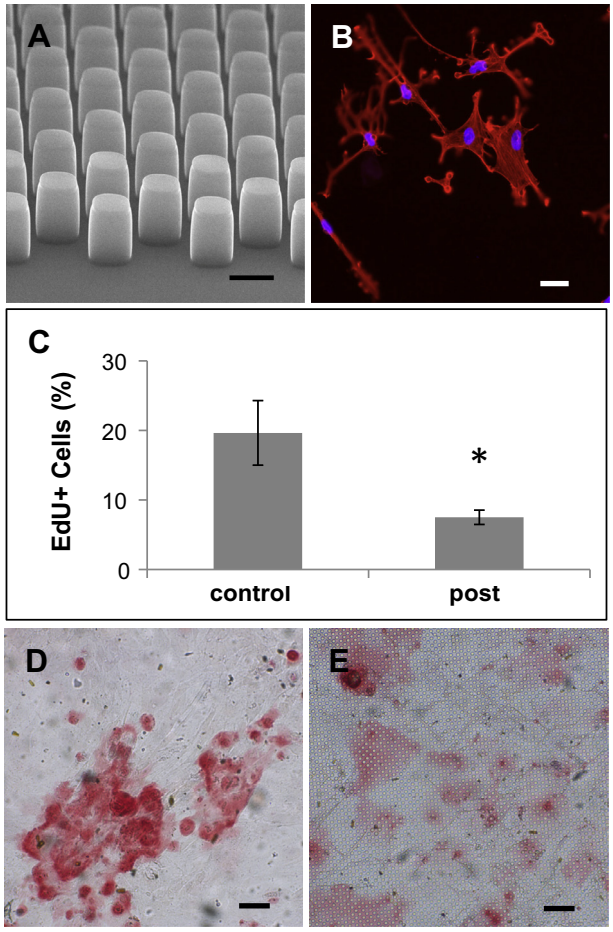

Fig. 4. VSC morphology, proliferation and calcified matrix deposition on micropost PDMS substrates. SEM of micropost PDMS surface (A). Cytoskeletal organization was verified with Alexa Phalloidin 546 staining and DAPI nuclear counterstaining (B). VSC proliferation on microposts was quantified using EdU incorporation assay (C). Alizarin red staining was used to stain calcified matrix deposition by VSC cultured in osteogenic media on control unpatterned PDMS (D) and on PDMS microposts (E). Scale bar = 5 μm (A), 50 μm (B, D and E). $^{*}p < 0.05$ compared to control. (For interpretation of the references to color in this figure legend, the reader is referred to the web version of this article.)

fibroblast proliferation on PDMS microposts while Mata et al., showed increased connective tissue progenitor (CTP) cell proliferation [20,21]. The differences in observation may be due to micropost size and spacing, and the morphology of the cells on the substrates. The CTP cells adhered to the PDMS in between the microposts while both the fibroblasts in the Green et al., study and the VSC in this study were primarily adhered on the post surfaces. Cell adhesion on the post surfaces may have decreased integrin–ligand interactions compared to cell adhesion on the flat surfaces in between microposts, and the reduced integrin–ligand interactions may have contributed to lower cell proliferation.

3.7. Micropost surfaces decreased calcified matrix deposition

Finally, we determined whether microposts were effective in reducing calcified matrix deposition of osteogenic VSC. After 4 weeks of culture on micropost surfaces in osteogenic medium, VSC showed substantially less alizarin red staining (Fig. 4E) as compared to control unpatterned PDMS (Fig. 4D). Similar to the decrease in proliferation, the decrease in calcified matrix deposition on microposts may be due to the interference in integrin–ligand interactions. While this study was not designed to assess substrate rigidity, it is likely that micropost rigidity played a role in modulating VSC proliferation and osteogenic differentiation.

Our results with microgrooved and micropost surfaces showed that microposts are effective in reducing both VSC proliferation and calcified matrix deposition. These results have important implications for the clinical performance of blood contacting cardiovascular implant devices. Micropost patterning of coronary stents or small diameter vascular grafts may improve blood vessel patency by reducing or preventing tissue restenosis and calcification. In order to translate these technologies to the clinic, cardiovascular implant studies in animal models are necessary to determine whether micropost patterning improves chronic implant performance.

Our findings also open new avenues for further investigation on the effect of micropatterned surfaces on VSC. Future studies will focus on determining whether micropost patterned surfaces modulate the differentiation of VSC into other lineages, and on the underlying molecular mechanisms responsible for altering VSC behavior.

Acknowledgments

The authors thank Mary West at the QB3 Stem Cell Culture Facility, Paul Lum at the Biomolecular Nanotechnology Center, and Dr. Song Li in the Department of Bioengineering for their assistance.

References

[1] N. Alexopoulos, P. Raggi, Calcification in atherosclerosis, Nat. Rev. Cardiol. 6 (2009) 681–688.
[2] R. Wessely, New drug-eluting stent concepts, Nat. Rev. Cardiol. 7 (2010) 194–203.
[3] S. Cassese, R.A. Byrne, T. Tada, S. Pinieck, M. Joner, T. Ibrahim, et al., Incidence and predictors of restenosis after coronary stenting in 10 004 patients with surveillance angiography, Heart 100 (2) (2013) 153–159.
[4] M.Y. Speer, H.Y. Yang, T. Brabb, E. Leaf, A. Look, W.L. Lin, et al., Smooth muscle cells give rise to osteochondrogenic precursors and chondrocytes in calcifying arteries, Circ. Res. 104 (2009) 733–741.
[5] Z. Tang, A. Wang, F. Yuan, Z. Yan, B. Liu, J.S. Chu, et al., Differentiation of multipotent vascular stem cells contributes to vascular diseases, Nat. Commun. 3 (2012) 875.
[6] E.T. den Braber, J.E. de Ruijter, H.T. Smits, L.A. Ginsel, A.F. von Recum, J.A. Jansen, Effect of parallel surface microgrooves and surface energy on cell growth, J. Biomed. Mater. Res. 29 (1995) 511–518.
[7] D.M. Brunette, Spreading and orientation of epithelial cells on grooved substrata, Exp. Cell Res. 167 (1986) 203–217.
[8] R.G. Thakar, Q. Cheng, S. Patel, J. Chu, M. Nasir, D. Liepmann, et al., Cell-shape regulation of smooth muscle cell proliferation, Biophys. J. 96 (2009) 3423–3432.
[9] T.L. Downing, J. Soto, C. Morez, T. Houssin, A. Fritz, F. Yuan, et al., Biophysical regulation of epigenetic state and cell reprogramming, Nat. Mater. 12 (2013) 1154–1162.
[10] J.L. Tan, J. Tien, D.M. Pirone, D.S. Gray, K. Bhadriraju, C.S. Chen, Cells lying on a bed of microneedles: an approach to isolate mechanical force, Proc. Natl. Acad. Sci. USA 100 (2003) 1484–1489.
[11] E.J. Kim, C.A. Boehm, A. Mata, A.J. Fleischman, G.F. Muschler, S. Roy, Post microtextures accelerate cell proliferation and osteogenesis, Acta Biomater. 6 (2010) 160–169.
[12] M.J. Dalby, N. Gadegaard, R. Tare, A. Andar, M.O. Riehle, P. Herzyk, et al., The control of human mesenchymal cell differentiation using nanoscale symmetry and disorder, Nat. Mater. 6 (2007) 997–1003.
[13] R.G. Thakar, F. Ho, N.F. Huang, D. Liepmann, S. Li, Regulation of vascular smooth muscle cells by micropatterning, Biochem. Biophys. Res. Commun. 307 (2003) 883–890.
[14] J. Fu, Y.K. Wang, M.T. Yang, R.A. Desai, X. Yu, Z. Liu, et al., Mechanical regulation of cell function with geometrically modulated elastomeric substrates, Nat. Methods 7 (2010) 733–736.
[15] R.D. Sochol, A.T. Higa, R.R.R. Janairo, S. Li, L.W. Lin, Unidirectional mechanical cellular stimuli via micropost array gradients, Soft Matter 7 (2011) 4606–4609.
[16] Y. Li, J.S. Chu, K. Kurpinski, X. Li, D.M. Bautista, L. Yang, et al., Biophysical regulation of histone acetylation in mesenchymal stem cells, Biophys. J. 100 (2011) 1902–1909.

[17] R. McBeath, D.M. Pirone, C.M. Nelson, K. Bhadriraju, C.S. Chen, Cell shape, cytoskeletal tension, and RhoA regulate stem cell lineage commitment, Dev. cell 6 (2004) 483–495.
[18] M.J. Dalby, D. McCloy, M. Robertson, C.D. Wilkinson, R.O. Oreffo, Osteoprogenitor response to defined topographies with nanoscale depths, Biomaterials 27 (2006) 1306–1315.
[19] M.J. Biggs, R.G. Richards, N. Gadegaard, C.D. Wilkinson, R.O. Oreffo, M.J. Dalby, The use of nanoscale topography to modulate the dynamics of adhesion formation in primary osteoblasts and ERK/MAPK signalling in STRO-1+ enriched skeletal stem cells, Biomaterials 30 (2009) 5094–5103.
[20] A.M. Green, J.A. Jansen, J.P. van der Waerden, A.F. von Recum, Fibroblast response to microtextured silicone surfaces: texture orientation into or out of the surface, J. Biomed. Mater. Res. 28 (1994) 647–653.
[21] A. Mata, C. Boehm, A.J. Fleischman, G. Muschler, S. Roy, Growth of connective tissue progenitor cells on microtextured polydimethylsiloxane surfaces, J. Biomed. Mater. Res. 62 (2002) 499–506.